

# Dislocation-limited open circuit voltage in film crystal silicon solar cells

Kirstin Alberi, Howard M. Branz, Harvey Guthrey, Manuel J. Romero, Ina T. Martin, Charles W. Teplin, Paul Stradins, and David L. Young  
National Renewable Energy Laboratory, Golden, Colorado 80401, USA

(Received 23 July 2012; accepted 6 September 2012; published online 21 September 2012)

Carrier recombination at dislocations is a major source of efficiency loss in epitaxial film Si solar cells and significantly affects the open circuit voltage,  $V_{OC}$ . We develop a simple empirical model that yields a logarithmic relationship between  $V_{OC}$  and the dislocation density, which fits well to our data. Straightforward evaluation of device performance with this model provides qualitative information about the recombination activity at dislocations. © 2012 American Institute of Physics. [<http://dx.doi.org/10.1063/1.4754142>]

Thin crystalline Si solar cells (2–10  $\mu\text{m}$  thick) fabricated on low-cost substrates have potential as a high efficiency, low-cost alternative to thin-film technologies currently competing with wafer-based devices in the photovoltaic marketplace. Film Si draws on the established scientific and manufacturing knowledge of the Si community while avoiding the cost of the wafer. Low-cost fabrication of film Si usually requires low crystal formation temperatures or handling of thin layers and normally causes a reduction in Si crystal quality compared with Si wafers. This includes increased concentrations of point defects and dislocations or even the incorporation of twins or grain boundaries, although at much lower defect densities than in thin-film polycrystalline or nanocrystalline Si.<sup>1–5</sup> It is therefore necessary to understand to what extent these tradeoffs in material quality affect device performance. In the case of unpassivated epitaxial films grown by hot-wire chemical vapor deposition (HWCVD) on a single crystalline seed template layer, we have shown previously that dislocations are the dominant recombination pathway and limit the effective minority carrier diffusion length,  $L_{eff}$ , when in the  $10^4$ – $10^7\text{ cm}^{-2}$  range.<sup>6</sup> This paper outlines the empirically determined relationship between open circuit voltage,  $V_{OC}$ , and dislocation density,  $N_d$ , in HWCVD epitaxial thin c-Si devices. These insights are then used to understand the performance-limiting mechanisms in a variety of film Si solar cells.

The experimental  $V_{OC}$  vs  $N_d$  relationship was assessed in 2  $\mu\text{m}$  thick c-Si cells grown by HWCVD at display-glass compatible temperatures ( $650 \leq T_G \leq 750^\circ\text{C}$ ) on heavily doped (arsenic:  $2 \times 10^{19}\text{ cm}^{-3}$ ) wafer substrates. The device structure is shown in Fig. 1. In a previous publication, we reported that the substrate temperature during growth,  $T_G$ , strongly influences the density of threading dislocations, so here we varied  $T_G$  to control  $N_d$ .<sup>7</sup> The n-type doping of the absorber was achieved intentionally through the flow of phosphine gas and/or unintentionally via redeposition of residual P in the growth chamber. The nominal doping density was determined by capacitance vs voltage (CV) measurements on completed cells to be roughly  $10^{16}\text{ cm}^{-3}$ , although exact values varied between devices. An i (3 nm)/p<sup>+</sup> (15 nm) hydrogenated amorphous silicon (a-Si:H) emitter was also formed by HWCVD, and the device was finished with a highly conductive indium tin oxide transparent front contact.

Details of the HWCVD epitaxial<sup>7–9</sup> and heterojunction<sup>10</sup> depositions can be found elsewhere. Post-deposition treatments, such as rapid thermal annealing or hydrogenation, as well as light trapping are typically used to enhance film c-Si device performance, however, none of these techniques were applied to the samples reported here. The  $V_{OC}$  was determined from current-voltage (JV) measurements, and  $N_d$  was ascertained by electron-beam induced current (EBIC) analysis on a FEI Nova600 field emission scanning electron microscope (FESEM) equipped with a Matelect EBIC picoamplifier. The  $L_{eff}$  values for minority carriers in the base region of the device were estimated using internal quantum efficiency (IQE) data.<sup>11–13</sup>

The experimental data displayed in Fig. 2(a) reveal a logarithmic relationship between  $V_{OC}$  and  $N_d$  for dislocation densities between  $10^5$  and  $10^7\text{ cm}^{-2}$ . Representative EBIC images for two of these devices are shown in Figs. 2(b) and 2(c). The measurements were carried out over areas up to  $100\text{ }\mu\text{m} \times 100\text{ }\mu\text{m}$  at several locations across each device in order to obtain meaningful statistical information, and  $N_d$  was found to remain relatively constant. Some degradation of the EBIC current was observed under the electron beam and is likely attributed to the charging of impurities in the epitaxial Si layers since similar behavior is not observed in Si heterojunction solar cell devices fabricated from high purity Si wafers (ITO/a-Si/c-Si/Al). This effect was minimized by performing the measurements under environmental conditions designed to release accumulated charge and utilizing fast scan speeds. The peak current loss at typical threading dislocations (dashed box in Fig. 2(c)) is approximately 10%–30%, as indicated by the EBIC intensity line scan

Device Structure

|  |                   |
|--|-------------------|
| ITO  | 60 nm             |
| a-Si:H heterojunction (i + p <sup>+</sup> )                | 18 nm             |
| n <sup>-</sup> epi absorber ( $10^{16}\text{ cm}^{-3}$ )   | 2 $\mu\text{m}$   |
| n <sup>+</sup> wafer template ( $10^{19}\text{ cm}^{-3}$ ) | 625 $\mu\text{m}$ |
| Ti/Ag/Pd Back Contact                                      |                   |

FIG. 1. Device structure.

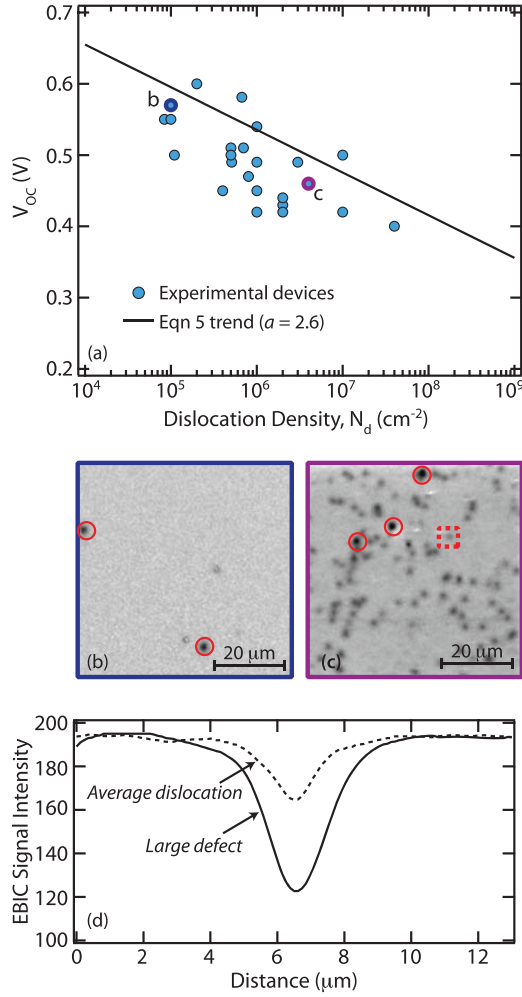


FIG. 2. (a) Experimental  $V_{OC}$  vs  $N_d$  data. The solid line represents the theoretical calculation from Eq. (5) with  $a = 2.6$ . The EBIC images in panels (b) and (c) correspond to the experimental points labeled in (a). (d) EBIC linescans through a typical dislocation (lighter spots similar to the one highlighted in the dashed square) with current loss of 10%–30% and a more complex defect (large dark spots in circles) with current loss of ~50%.

(dotted line) displayed in Fig. 2(d). The corresponding device characteristics are given in Table I. Temperature-dependent EBIC measurements (79 K–300 K) reveal that this relatively high contrast at the dislocations is constant throughout this temperature range. This suggests that high concentrations of metal impurities decorate the dislocations with a linear density of deep levels exceeding  $10^7 \text{ cm}^{-1}$  according to an estimate from the recombination model developed by Kveder *et al.*<sup>14</sup> Clean or slightly decorated dislocations with a linear density of deep levels below  $10^6 \text{ cm}^{-1}$  would have an EBIC contrast with a very pronounced

TABLE I. Device characteristics of cells with EBIC shown in Figs. 2(b) and 2(c).

| Cell | $V_{OC}$ (V) | $J_{SC}$ ( $\text{mA}/\text{cm}^2$ ) | FF (%) | Eff (%) | Dislocation density ( $\text{cm}^{-2}$ ) | Growth temperature ( $^{\circ}\text{C}$ ) |
|------|--------------|--------------------------------------|--------|---------|--|---|
| b    | 0.57         | 15.3                                 | 72.5   | 6.3     | $1\text{E}5$                             | 760                                       |
| c    | 0.46         | 10.0                                 | 68.9   | 3.2     | $4\text{E}6$                             | 700                                       |

temperature-dependence, which is not observed in these films. Metal contamination in the devices presented in Ref. 6 and this paper could be introduced from the hot W filament during HWCVD growth. If each dislocation was decorated with  $10^7 \text{ cm}^{-1}$  metal atoms, then a dislocation density of  $10^6 \text{ cm}^{-2}$  would yield a total metal impurity density of  $10^{13} \text{ cm}^{-3}$ . However, this density is below the secondary ion mass spectrometry (SIMS) detection limit for W ( $\sim 10^{15} \text{ cm}^{-3}$ ), which showed no evidence for any metal at higher concentrations. These results suggest that the bulk material in between dislocations does not contain high concentrations ( $> 10^{15} \text{ cm}^{-3}$ ) of metal impurities.<sup>15</sup>

The logarithmic relationship between  $V_{OC}$  and  $N_d$  can be understood as a consequence of minority carrier recombination at dislocations.  $V_{OC}$  is governed by the splitting of the electron and hole quasi-Fermi levels ( $E_{Fn}$  and  $E_{Fp}$ , respectively)

$$qV_{OC} = E_{Fn} - E_{Fp} = kT \ln \left( \frac{np}{n_i^2} \right). \quad (1)$$

Under illumination, the majority electron concentration ( $n$ ) in the absorber does not change significantly; in contrast, the minority hole concentration ( $p$ ) depends on their lifetime ( $\tau$ ) and the rate ( $G$ ) at which holes are photogenerated

$$p = G\tau. \quad (2)$$

We previously reported that the hole minority carrier lifetime in these film c-Si devices epitaxially grown on wafer substrates is limited mainly by recombination at dislocations.<sup>6</sup> Several models have been developed to quantify the effects of dislocations on  $\tau$  and  $L_{eff}$  in Si solar cells.<sup>16–18</sup> Most notably, Donolato developed a rigorous analytical model of  $L_{eff}$  based on the charge collection probability in a specimen with a 2D array of regularly spaced dislocations.<sup>16</sup> Here, we establish this dependence empirically by plotting  $L_{eff}$  as a function of distance between dislocations ( $1/\sqrt{N_d}$ ) in Fig. 3. The relationship between the two can generally be expressed as

$$L_{eff} = \frac{1}{a\sqrt{N_d}}, \quad (3)$$

where the dimensionless parameter  $a$  is a measure of how strongly dislocations affect recombination. A value of  $a \sim 2.6 \pm 0.2$  was determined from the slope of the experimental best-fit line shown in Figure 3. Qualitatively, low  $a$  values suggest that a small capture cross-section for carriers recombination at dislocations, while high  $a$  values indicate a large capture cross-section.

By combining Eqs. (2) and (3) with  $\tau = L_{eff}^2/D_p$ , we find that  $p$  is inversely related to  $N_d$

$$p = G\tau = \frac{GL_{eff}^2}{D_p} = \frac{G}{a^2 N_d D_p}, \quad (4)$$

where  $D_p$  is the hole diffusivity. Inserting Eq. (4) into Eq. (1), the final expression for  $V_{OC}$  as a function of  $N_d$  can be written as

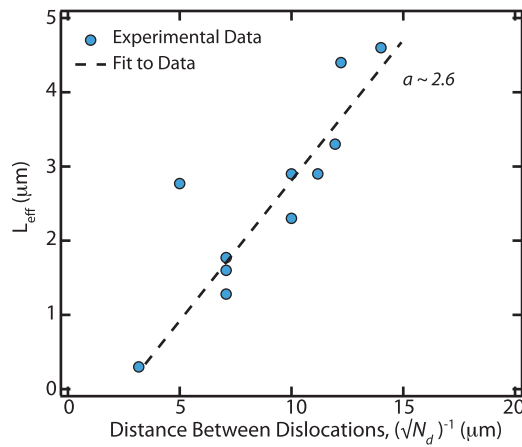


FIG. 3. Effective diffusion length ( $L_{eff}$ ) vs distance between dislocations  $(\sqrt{N_d})^{-1}$ . The slope to the best-fit line to Eq. (3) yields a value of  $a = 2.6 \pm 0.2$ .

$$V_{OC} = \frac{kT}{q} \ln \left( \frac{nG}{N_d a^2 D_p n_i^2} \right). \quad (5)$$

We estimated a generation rate of  $G = 2 \times 10^{20} \text{ cm}^{-3}$  from the amount of light absorbed in a  $2 \mu\text{m}$  thick Si layer. The solid theoretical line plotted in Fig. 2(a) then represents the Eq. (5) relationship between  $V_{OC}$  and  $N_d$  for  $a = 2.6$  and  $n \sim 10^{16} \text{ cm}^{-3}$ . A room temperature  $kT$  slope ( $0.026 \text{ eV}$ ) and the standard Si  $D_p = 10 \text{ cm}^2 \text{ s}^{-1}$  and  $n_i = 1.3 \times 10^{10} \text{ cm}^{-3}$  values were assumed in the calculation. This theoretical trend line marks a moderate upper bound to the experimental  $V_{OC}$  vs  $N_d$  dependence and supports the finding that  $a \sim 2.6$  is the characteristic of HWCVD thin film Si devices in which  $L_{eff}$  is limited by unpassivated dislocations with moderate current loss (10%–30% EBIC contrast).

In many of our devices, mechanisms other than recombination at dislocations affect  $V_{OC}$ , which often cause it to fall below the Eq. (5) prediction in Fig. 2(a) based upon dislocations alone. The EBIC micrographs shown in Fig. 2(b) also exhibit areas of more significant current loss ( $\sim 50\%$ ) associated with complex structural defects such as pits and stacking faults.<sup>19</sup> Examples of these larger and much darker defects are circled in Figs. 2(b) and 2(c), and a line scan of the typical current loss at these regions is shown in Fig. 2(d). In addition to acting as recombination sites, these areas can break down at much lower reverse bias than defect-free regions and act as shunt paths.<sup>20</sup> We observe the densities of these defects to be in the low  $10^4 \text{ cm}^{-2}$  range. They will induce some drop in the  $V_{OC}$  even when their concentration is well below that of the threading dislocations; when the concentrations are comparable, the shunts will likely limit  $V_{OC}$ .

A mixture of junction transport mechanisms and elevated space charge recombination is also expected to reduce the  $V_{OC}$ .<sup>21</sup> Most of these devices have relatively high dark saturation currents ( $J_0 \sim 10^{-7} \text{ A/cm}^2$ ) and ideality factors ( $n \sim 1.7$ ), which are likely due to recombination at poorly passivated defects near the heterojunction interface.<sup>6,21</sup> An average drop in the  $V_{OC}$  due to the high  $J_0$  is calculated to be roughly  $20 \text{ meV}$ . Lastly, scatter in the data can be produced by several sources, including variation in the absorber doping density and the metal-induced recombination activity at

unpassivated dislocations, which manifests as differences in EBIC contrast for different defects (see Fig. 2(c)).

The  $V_{OC}$  vs.  $N_d$  relationship of Eq. (5) provides a useful guide for understanding the losses in dislocation-limited epitaxial c-Si cells. A short discussion of  $a$  is warranted here in order to extract meaningful information from the fit. This parameter incorporates many factors that are explicitly treated by the detailed models in Refs. 16–18 into one experimentally accessible term. These factors include the inherent diffusion length of the bulk material without dislocations, the effective radius over which the dislocation can affect carrier recombination and its line recombination velocity. The parameter,  $a$ , can thus be viewed as a measure of the influence of dislocations on  $L_{eff}$  and can be used to parameterize their impact on recombination.

The analysis outlined above may be implemented to understand possible sources of  $V_{OC}$  loss in film c-Si solar cells as well as identify potential avenues for reducing them. High  $a$  values  $> 1$  indicate that dislocations are a major problem. Low  $a$  values or  $V_{OC}$  values that fall well below the Eq. (5) trend line may suggest that another factor is largely limiting the device performance. Evaluation of  $a$  can also be a simple approach to optimize device fabrication conditions. For example, reduction in the recombination activity at dislocations in the devices presented here can be achieved by decreasing the degree of metal decoration on the dislocations or by passivating these recombination sites. Initial results suggest that standard post-deposition hydrogenation treatments lower  $a$  through the second approach.<sup>21,22</sup> This effect is particularly evident in devices containing high dislocation densities, where the incorporation of a hydrogenation step has produced a film-Si solar cell with  $L_{eff} = 4.5 \mu\text{m}$  and  $V_{OC} = 0.57 \text{ V}$  despite  $N_d = 10^8 \text{ cm}^{-2}$ .<sup>22</sup> Inserting these values into Eq. (5) suggests that the hydrogenation step has dropped  $a$  to  $\sim 0.4$  even though the dislocation density was not changed. Post-deposition treatment conditions could be further optimized by minimizing  $a$ .

In conclusion, this straightforward approach based upon simple device measurements can be applied to understand the relative effects of dislocations on the performance of thin film c-Si solar cells. The  $V_{OC}$  should follow a logarithmic relationship with  $N_d$  when dislocations are the primary limiter of device efficiency. An empirically determined  $a$  parameter can also be used to assess the recombination activity at dislocations.

This work was supported by the U.S. DOE Solar Energy Technology Program under Contract No. DE-AC3608GO28308. The authors thank C. Beall, M. Shub, L. Roybal, A. Duda, and the late E. Iwaniczko for their technical help in device fabrication.

<sup>1</sup>A. G. Aberle, A. Straub, P. I. Widenborg, A. B. Sproul, Y. Huang, and P. Campbell, *Prog. Photovoltaics* **13**, 37 (2005).

<sup>2</sup>K. Van Nieuwenhuysen, F. Duerinckx, I. Kuzma, D. van Gestel, G. Beaucarne, and J. Poortmans, *J. Cryst. Growth* **287**, 438 (2006).

<sup>3</sup>M. J. Keevers, T. L. Young, U. Schubert, and M. A. Green, in *Proceedings of the 22nd European Photovoltaic Solar Energy Conference and Exhibition (EUPVSEC)*, Milan (2007), p. 1783.

<sup>4</sup>P. Dogan, E. Rudigier, F. Fenske, K. Y. Lee, B. Gorka, B. Rau, E. Conrad, and S. Gall, *Thin Solid Films* **516**, 6989 (2008).

<sup>5</sup>I. Gordon, S. Vallon, A. Mayolet, G. Beaucarne, and J. Poortmans, *Sol. Energy Mater. Sol. Cells* **94**, 381 (2010).

- <sup>6</sup>K. Alberi, I. T. Martin, M. Shub, C. W. Teplin, M. J. Romero, R. C. Reedy, E. Iwaniczko, A. Duda, P. Stradins, H. M. Branz, and D. L. Young, *Appl. Phys. Lett.* **96**, 073502 (2010).
- <sup>7</sup>C. W. Teplin, K. Alberi, M. Shub, C. Beall, I. T. Martin, M. J. Romero, D. L. Young, R. C. Reedy, P. Stradins, and H. M. Branz, *Appl. Phys. Lett.* **96**, 201901 (2010).
- <sup>8</sup>H. M. Branz, C. W. Teplin, M. J. Romero, I. T. Martin, Q. Wang, K. Alberi, D. L. Young, and P. Stradins, *Thin Solid Films* **519**, 4545 (2011).
- <sup>9</sup>I. T. Martin, H. M. Branz, P. Stradins, D. L. Young, R. C. Reedy, and C. W. Teplin, *Thin Solid Films* **517**, 3496 (2009).
- <sup>10</sup>Q. Wang, M. R. Page, E. Iwaniczko, Y. Q. Xu, L. Roybal, R. Bauer, B. To, H. C. Yuan, A. Duda, F. Hasoon, Y. F. Fan, D. Levi, D. Meier, H. M. Branz, and T. H. Wang, *Appl. Phys. Lett.* **96**, 013507 (2010).
- <sup>11</sup>P. A. Basore, in *IEEE PVSC-23* (IEEE, 1993).
- <sup>12</sup>R. Brendel, M. Hirsch, M. Stemmer, U. Rau, and J. H. Werner, *Appl. Phys. Lett.* **66**(10), 1261 (1995).
- <sup>13</sup>K. Taretto, U. Rau, and J. H. Werner, *J. Appl. Phys.* **93**(9), 5447 (2003).
- <sup>14</sup>V. Kveder, M. Kittler, and W. Schroter, *Phys. Rev. B* **63**, 115208 (2001).
- <sup>15</sup>Internal quantum efficiency data, presented in Ref. **6**, demonstrate efficient carrier collection from the back of those devices with relatively low dislocation densities. This suggests that bulk impurities do not limit recombination within these thin devices.
- <sup>16</sup>C. Donolato, *J. Appl. Phys.* **84**, 2656 (1998).
- <sup>17</sup>C. van Opdorp, A. T. Vink, and C. Werkhoven, in *Proceedings of the 6th III-V Symposium, St. Louis, MO, 1976*, edited by L. F. Eastman, Inst. Phys. Conf. Ser. 33b (Institute of Physics, Bristol, 1977), p. 317.
- <sup>18</sup>M. Lax, *J. Appl. Phys.* **49**, 2796 (1978).
- <sup>19</sup>H. R. Moutinho, D. L. Young, C. W. Teplin, K. Alberi, C.-S. Jiang, and M. M. Al-Jassim, in *IEEE-PVSC* (IEEE, Seattle, WA, 2011).
- <sup>20</sup>M. J. Romero, K. Alberi, I. T. Martin, K. M. Jones, D. L. Young, Y. Yan, C. W. Teplin, M. M. Al-Jassim, P. Stradins, and H. M. Branz, *Appl. Phys. Lett.* **97**, 092107 (2010).
- <sup>21</sup>D. L. Young, J. V. Li, C. W. Teplin, P. Stradins, and H. M. Branz, in *IEEE PVSC* (IEEE, Seattle, 2011).
- <sup>22</sup>C. W. Teplin, B. Lee, T. R. Fanning, J. Wang, S. Grover, F. Hasoon, R. Bauer, J. Bornstein, P. Schroeter, and H. M. Branz, *Energy Environ. Sci.* **5**, 8193 (2012).